



HAL
open science

Polarized signal singular spectrum analysis with complex SSA

Sébastien Journé, Nicolas Le Bihan, Florent Chatelain, Julien Flamant

► **To cite this version:**

Sébastien Journé, Nicolas Le Bihan, Florent Chatelain, Julien Flamant. Polarized signal singular spectrum analysis with complex SSA. ICASSP 2023 - IEEE International Conference on Acoustics, Speech and Signal Processing, Jun 2023, Rhodes Island, Greece. 10.1109/ICASSP49357.2023.10095954 . hal-04104834

HAL Id: hal-04104834

<https://hal.science/hal-04104834>

Submitted on 18 Jun 2023

HAL is a multi-disciplinary open access archive for the deposit and dissemination of scientific research documents, whether they are published or not. The documents may come from teaching and research institutions in France or abroad, or from public or private research centers.

L'archive ouverte pluridisciplinaire **HAL**, est destinée au dépôt et à la diffusion de documents scientifiques de niveau recherche, publiés ou non, émanant des établissements d'enseignement et de recherche français ou étrangers, des laboratoires publics ou privés.

POLARIZED SIGNAL SINGULAR SPECTRUM ANALYSIS WITH COMPLEX SSA

*Sébastien Journé**, *Nicolas Le Bihan**, *Florent Chatelain**, *Julien Flamant†*

*Univ. Grenoble Alpes, CNRS, Grenoble INP, GIPSA-lab, 38000 Grenoble France

†Université de Lorraine, CNRS, CRAN, F-54000 Nancy, France

ABSTRACT

This paper considers the analysis of bivariate signals using complex Singular Spectrum Analysis (SSA). It introduces a pseudo-correlation based criterion in the grouping step of complex SSA. The advantage of using pseudo-correlation rather than correlation measures when analyzing polarized signals with complex SSA is demonstrated theoretically. This criterion is shown to be effective to extract bivariate signals modeled as particular complex Linear Recurrence Relations (LRR) of order 2. These elementary complex bricks offer a high interpretability in terms of polarization. Illustration of the proposed grouping technique is made through polarized component extraction on a real-world data example.

Index Terms— Singular Spectrum Analysis, Bivariate Signals, Polarization, Linear Recurrence Relation, Pseudo-Correlation criterion

1. INTRODUCTION

Bivariate signals can be found in many fields such as optics [1], [2], seismology [3], [4], gravitational wave astrophysics [5, 6] or physical oceanography [7], [8] to name just a few. For such physical applications, the notion of polarization plays a key role: it encodes the geometry of oscillations in the 2D plane. More intuitively, it can be seen as the signal trajectory in the complex plane. The analysis of the evolution of polarization with respect to time, space or frequency enables many fundamental insights about the underlying physics. As an example, Figure 1 shows a seismic bivariate signal: while its two components have similar dynamic content, its trajectory in the 2D plane takes the form of a slowly evolving ellipse. Thus, it defines an elliptically polarized (bivariate) signal and reveals the geophysical nature of the wave, in that case a Rayleigh wave. Recent works [9, 10] have further shown that polarization has a general relevance for the analysis and filtering of bivariate signals. However, current approaches do not yield simple bivariate signal models that have a straightforward interpretation in terms of polarization.

To this aim, this paper introduces an elementary discrete-time bivariate signal model that enables interpretation in terms of polarization. In this paper, the complex representation of a bivariate signal is used rather than its 2D real vector representation, as it allows notably for direct definitions of amplitude and phase [11, 12]. To construct the model, one considers rank-1 matrices obtained from the complex-valued Hankel matrix built from a bivariate signal, with the help of the Complex Singular Spectrum Analysis (SSA). Signals obtained from rank-1 matrices are recombined into elementary components interpretable polarization-wise. The main contribution of this paper consists in the introduction of low-rank elementary polarized components together with the proposition of a dedicated crite-

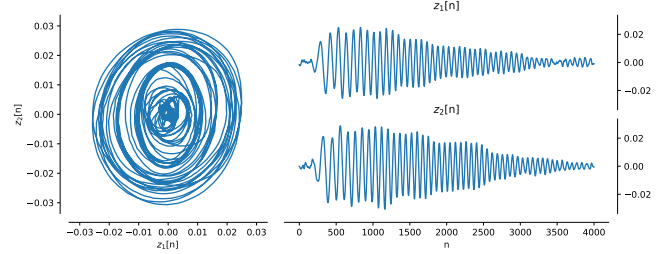


Fig. 1: Bivariate signal example: seismic displacement along the horizontal and vertical axes from the 1991 Solomon Islands Earthquake (normalized) available online [13].

riterion to combine elementary polarized components obtained via the SSA decomposition.

2. PRELIMINARIES

Notations. Vectors and matrices are denoted in bold lowercase and uppercase letters, respectively. The complex conjugate of $\alpha \in \mathbb{C}$ is denoted as $\bar{\alpha}$. The transpose conjugate of a matrix M is M^\dagger and its rank is given by $\text{rk } M$. Throughout the paper we use the complex vector $\mathbf{z} \in \mathbb{C}^N$ to denote a discrete bivariate signal of length N , defined in terms of its real-valued components $\mathbf{z}_1, \mathbf{z}_2 \in \mathbb{R}^N$ such that $z[n] = z_1[n] + iz_2[n]$ for $n = 0, \dots, N-1$ where $i^2 = -1$.

Complex SSA. Standard real-valued SSA is a well established univariate time-series analysis tool that has been shown to provide efficient signal denoising or trend extraction methods [14]. It relies on low-rank decomposition of Hankel matrix embeddings of time-series through the use of the singular value decomposition (SVD). It can be extended to complex and multivariate signals [15]. We recall below the different steps of complex SSA:

1. The signal $\mathbf{z} \in \mathbb{C}^N$ is embedded into a Hankel matrix \mathbf{H} with a user-defined number of L rows,

$$\mathbf{H} = \begin{pmatrix} z[0] & z[1] & z[2] & \dots & z[K-1] \\ z[1] & z[2] & \dots & \dots & z[K] \\ z[2] & \dots & \dots & \dots & z[K+1] \\ \dots & \dots & \dots & \dots & \dots \\ z[L-1] & z[L] & z[L+1] & \dots & z[N-1] \end{pmatrix} \in \mathbb{C}^{L \times K}, \quad (1)$$

where $K = N - L + 1$.

2. Compute the rank- r truncated SVD $\mathbf{H} = \sum_i^r \mathbf{H}_i$, with $\mathbf{H}_i = \sigma_i \mathbf{u}_i \mathbf{v}_i^\dagger$ where σ_i is the i^{th} singular value in descending order, \mathbf{u}_i and \mathbf{v}_i are the corresponding left and right singular vectors.

3. Recover the r elementary components $\mathbf{s}_i \in \mathbb{C}^N$ by anti-diagonal averaging of the rank-1 matrices $\mathbf{H}_i \in \mathbb{C}^{L \times K}$ (we will refer to it as the *anti-diagonal averaging* process). Precisely, the n^{th} term $s_i[n]$ is defined as the average of the n^{th} anti-diagonal of \mathbf{H}_i .
4. The last step, known as the *grouping* step, consists in finding a partition of the set of r elementary time-series $\{\mathbf{s}_i\}_{1 \leq i \leq r}$ to perform a given task, such as extracting trends or denoising [14]. This is usually carried out by clustering analysis of pairwise correlations between elementary components.

Compared to the classical SSA, the 3rd step on *anti-diagonal averaging* and the 4th step on grouping are swapped. Working on time-series rather than matrices leads to easier grouping.

3. THE CONSTRAINED LINEAR RECURRENCE RELATION OF ORDER 2

3.1. Linear Recurrence Relation (LRR) models

As explained in [16], the SSA procedure is particularly adapted to the analysis of signals defined by Linear Recurrence Relation (LRR) models. It actually revolves around a central property of Hankel matrices: for a proper choice of the window length L , if $\text{rk } \mathbf{H} = r \leq \min(L, K)$, the time-series generating \mathbf{H} follows a LRR of order r . Working with LRRs as elementary components of the SSA makes it more amenable to further analysis and theoretical results compared to data-driven approaches.

A complex-valued LRR of order r explicitly reads:

$$z[n+r] = \lambda_1 z[n+r-1] + \lambda_2 z[n+r-2] + \dots + \lambda_r z[n], \quad (2)$$

for any $n \in \mathbb{N}$, with $\lambda_i \in \mathbb{C}$ for $1 \leq i \leq r$. From (2) with $r = 1$, the following closed-form expression stands for a LRR of order 1:

$$z[n] = x_0 \lambda^n, \quad (3)$$

with $x_0, \lambda \in \mathbb{C}$ and $\lambda = \lambda_1$ from (2). This is the most elementary complex-valued LRR. It generates a rank-1 Hankel matrix.

3.2. Constrained LRR2

Of central interest in the sequel is a special type of second order complex-valued LRR, denoted *constrained LRR2*. It is defined as follows.

Definition 3.1. A *constrained LRR2* is defined as:

$$z[n] = x_0 \lambda^n + y_0 \bar{\lambda}^n, \quad (4)$$

with $x_0, y_0 \in \mathbb{C}, \lambda \in \mathbb{C} \setminus \mathbb{R}$.

This definition is the sum of two LRR1 with opposite arguments, which means that the two complex time-series rotate in opposite directions in the complex plane. It is derived from the following special case of LRR2 equation:

$$z[n+2] = (\lambda + \bar{\lambda})z[n+1] - |\lambda|^2 z[n].$$

This highlights that a complex-valued LRR2 is *constrained* if and only if the weights in the LRR equation (2) obey the following: $\lambda_1, \lambda_2 \in \mathbb{R}, \lambda_2 < 0$ and $\lambda_1^2 < -4\lambda_2$. Note that any LRR1 (3) can be written as a constrained LRR2 by setting $y_0 = 0$ in (4). Only constrained LRR2 are considered in the sequel.

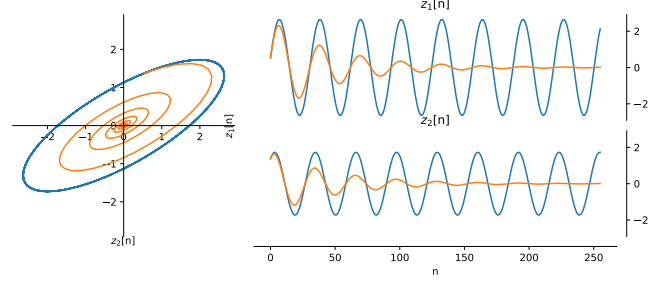


Fig. 2: Polarization interpretation of constrained LRR2. Two values of λ are shown: $|\lambda| = 1$ (blue) and $|\lambda| < 1$ (orange).

3.3. Polarization properties of constrained LRR2

Figure 2 depicts an example of a constrained LRR2 (4) with initial conditions $x_0 = e^{-i\frac{\pi}{12}}, y_0 = e^{i\frac{15\pi}{24}}$. Two values of λ are shown, of same argument $\arg \lambda = 0.2$ and different modulus $|\lambda| = 1$ (blue curve) and $|\lambda| = 0.98$ (orange curve). A constrained LRR2 with $|\lambda| = 1$ traces out an ellipse along time. This illustrates that constrained LRR2 are closely related to the trajectory in the 2D plane of a polarized (bivariate) signal. The *polarization ellipse* is usually characterized by four parameters [17] depending only on x_0 and y_0 :

$$\begin{aligned} a &= \sqrt{2} \sqrt{|x_0|^2 + |y_0|^2}, & \varphi &= \frac{\arg(x_0) - \arg(y_0)}{2}, \\ \theta &= \frac{\arg(x_0) + \arg(y_0)}{2}, & \tan \chi &= \frac{|x_0| - |y_0|}{|x_0| + |y_0|}. \end{aligned} \quad (5)$$

Here $a \geq 0$ is the amplitude or size of the ellipse, $\varphi \in [0, 2\pi)$ is the initial phase, $\theta \in [-\frac{\pi}{2}, \frac{\pi}{2}]$ is the *orientation*, giving the angle between the major axis of the ellipse and the horizontal axis, and $\chi \in [-\frac{\pi}{4}, \frac{\pi}{4}]$ is the *ellipticity* defining the shape of the ellipse. This last parameter is related to a ratio between the minor and major axis of the ellipse. For a value of $\chi = 0$, the ellipse is a line segment whereas for $\chi = \pm \frac{\pi}{4}$ it is a circle. For any χ in between it is an ellipse. Those cases are called respectively linearly, circularly and elliptically polarized. The sign of χ also dictates the running direction of the ellipse (positive is counter-clockwise and negative is clockwise). When $|\lambda| < 1$, the ellipse preserves its geometry, but its amplitude decreases with time, as seen in Figure 2.

This example shows that constrained LRR2 (4) have a straightforward interpretation in terms of polarization. Therefore, they appear as good candidates to form the elementary bricks in bivariate signals decomposition problems. In particular, identifying such components with complex SSA requires a dedicated grouping criterion, described in the next section.

4. A NEW GROUPING CRITERION: THE PSEUDO-CORRELATION

In the SSA procedure, the grouping step usually consists in grouping the *anti-diagonal averaged* rank-1 components into sets corresponding to interpretable signals. This is classically done using correlation measures [14]. In this section we introduce the pseudo-correlation as a way to identify constrained LRR2 in the SSA components. Let \mathbf{x}, \mathbf{y} two vectors in \mathbb{C}^N and $\rho(\mathbf{x}, \mathbf{y})$ denotes their correlation coefficient.

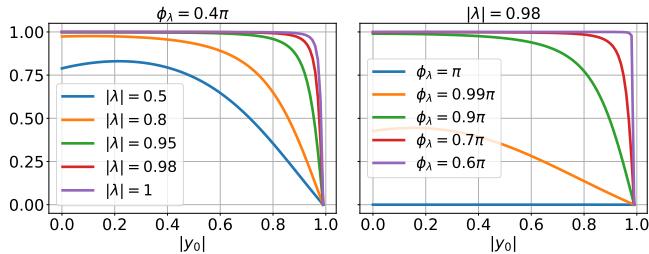


Fig. 3: Pseudo-correlation $|\tilde{\rho}(\mathbf{u}_1, \mathbf{u}_2)|$ as defined in Theorem 4.1 as a function of $|y_0|$ for a fixed $x_0 = e^{i0.6\pi}$ and $\phi_{y_0} = 1.4\pi$. Left: fixed phase of λ ($\phi_\lambda = 0.4\pi$) for a varying $|\lambda|$. Right: fixed $|\lambda| = 0.98$ for a varying phase ϕ_λ .

cient. Their pseudo-correlation $\tilde{\rho}(\mathbf{x}, \mathbf{y})$ is defined as:

$$\tilde{\rho}(\mathbf{x}, \mathbf{y}) = \rho(\mathbf{x}, \bar{\mathbf{y}}) = \frac{\sum_{n=0}^{N-1} x[n]y[n]}{\sqrt{\sum_{n=0}^{N-1} |x[n]|^2} \sqrt{\sum_{n=0}^{N-1} |y[n]|^2}}. \quad (6)$$

In the rest of this section we will discuss the advantages of this similarity measure to identify constrained LRR2. One can see after the second step of the SSA that the eigenvectors are by construction orthogonal, i.e., their correlation is zero, but their pseudo-correlation can still be non-zero. Such non-vanishing pseudo-correlations reveal polarization information shared by these eigenvectors. Consequently, a grouping criterion based on correlation can not guarantee to associate components forming polarized components while pseudo-correlation has the ability to do so.

4.1. Theoretical effectiveness of the pseudo-correlation

The rationale to use pseudo-correlation as a grouping criterion is that the two rank-1 components of a constrained LRR2 $x[n] = x_0\lambda^n$ and $y[n] = y_0\bar{\lambda}^n$ (4) are perfectly pseudo-correlated, i.e., $|\tilde{\rho}(\mathbf{x}, \mathbf{y})| = 1$. Then, if the SSA process is accurate enough, its output components are close enough to the two LRR1 inputs and should also be strongly pseudo-correlated. Theorem 4.1 allows us to quantify the pseudo-correlation between the SSA singular vectors.

Theorem 4.1. *Let $z[n] = x_0\lambda^n + y_0\bar{\lambda}^n$, for $n = 0, \dots, N-1$, be a constrained LRR2 signal as defined in (4). Then the pseudo-correlation between \mathbf{u}_1 and \mathbf{u}_2 (the first 2 left singular vectors obtained in the second step of the SSA) reads*

$$|\tilde{\rho}(\mathbf{u}_1, \mathbf{u}_2)| = (|x_0|^2 - |y_0|^2) f_K(|\lambda|) \sqrt{\frac{f_L(|\lambda|)^2 - |f_L(\lambda)|^2}{\delta}}, \quad (7)$$

with $f_M(a) = \sum_{m=0}^{M-1} a^{2m}$, and

$$\delta = [(|x_0|^2 + |y_0|^2) f_L(|\lambda|) f_K(|\lambda|) + 2\Re(x_0\bar{y}_0 f_L(\lambda) f_K(\lambda))]^2 - 4|x_0 y_0|^2 (f_L(|\lambda|)^2 - |f_L(\lambda)|^2) (f_K(|\lambda|)^2 - |f_K(\lambda)|^2).$$

Sketch of Proof. Following the method proposed in [14, p. 247], we derive \mathbf{u}_1 and \mathbf{u}_2 by computing the eigen-decomposition of a carefully designed complex matrix of dimension $r \times r$, where $r = 2$ corresponds to the rank of the Hankel matrix in step 1 of SSA. Straightforward computations yield their pseudo-correlation (7). \square

Theorem 4.1 can now be specialized for the limit values of the ellipticity parameter χ defined in (5).

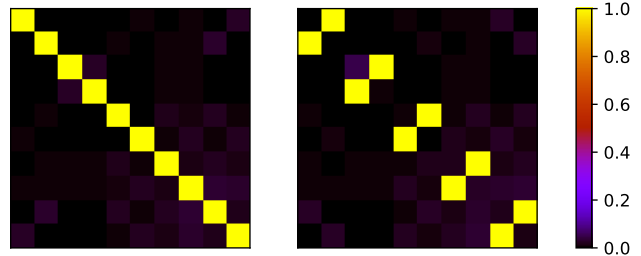


Fig. 4: Pairwise correlation (left) and pseudo-correlation (right) of the first 10 SSA components $\mathbf{s}_1, \dots, \mathbf{s}_{10}$ ($N = 2048$ and $L = 512$). The original signal is a sum of five constrained LRR2 whose parameters $|x_0|$ and $|y_0|$ are uniformly drawn in $[0; 10]$, $|\lambda|$ in $[0.95; 1]$ and $\arg \lambda$ in $[0; \pi)$.

Corollary 4.1 (Circular polarization). *Under the assumptions of Theorem 4.1, as $|\chi| \rightarrow \frac{\pi}{4}$, one has*

$$|\tilde{\rho}(\mathbf{u}_1, \mathbf{u}_2)| \xrightarrow{|\chi| \rightarrow \frac{\pi}{4}} \sqrt{1 - \frac{|f_L(\lambda)|^2}{f_L(|\lambda|)^2}}.$$

Corollary 4.1 shows the effectiveness of the pseudo-correlation when χ is close to $\pm \frac{\pi}{4}$, i.e., for grouping elliptically or circularly polarized components. In fact, for typical values of $\lambda \in \mathbb{C} \setminus \mathbb{R}$ with $|\lambda| \approx 1$, the singular vectors are shown to be almost perfectly pseudo-correlated ($|\tilde{\rho}(\mathbf{u}_1, \mathbf{u}_2)| \approx 1$) in case of (almost) circular polarization. These singular vectors are obtained in the second step of the SSA. Then, after an anti-diagonal averaging, the output of the third step of the SSA is \mathbf{s}_1 and \mathbf{s}_2 . But if \mathbf{u}_1 and \mathbf{u}_2 are perfectly pseudo-correlated, \mathbf{s}_1 and \mathbf{s}_2 are perfectly pseudo-correlated as well.

Corollary 4.2 (linear polarization). *Let \mathbf{s}_1 and \mathbf{s}_2 be the first 2 components obtained in the third step of SSA. Under the assumptions of Theorem 4.1, as $\chi \rightarrow 0$, one has*

$$|\tilde{\rho}(\mathbf{s}_1, \mathbf{s}_2)| \xrightarrow{\chi \rightarrow 0} |\rho(\mathbf{s}_1, \mathbf{s}_2)|,$$

where $\rho(\mathbf{s}_1, \mathbf{s}_2)$ is the correlation between \mathbf{s}_1 and \mathbf{s}_2 .

Corollary 4.2 shows now that pseudo-correlation becomes equivalent to the usual correlation criterion for linearly polarized components. Note that correlation is already used as a standard criterion for grouping the components associated with a linearly polarized input signal such that a (real) monochromatic signal $z[n] \propto \cos \omega n$ as detailed in [16]. Even if singular vectors are no longer pseudo-correlated in case of linear polarization, both correlations on the SSA components after *anti-diagonal averaging* can be quite high. To decode the polarization information of the signal, the correlation is only useful for linearly polarized signals. For circularly and elliptically polarized signals, the pseudo-correlation shows better performances while also being equivalent for linear polarization.

4.2. Numerical effectiveness of the pseudo-correlation

Figure 3 depicts the pseudo-correlation as given in Theorem 4.1 and Corollary 4.1 when $|y_0| \rightarrow 0$. As long as $|x_0| \neq |y_0|$ and the bivariate signal is not degenerate (i.e., $\arg(\lambda) \neq k\pi$) the modulus of the pseudo-correlation is close to 1 most of the time. This illustrates that it is a powerful criterion to group SSA components for elliptically polarized LRR2.

Figure 4 depicts pairwise correlations and pseudo-correlations between the SSA components obtained for a sum of LRR2 signals.

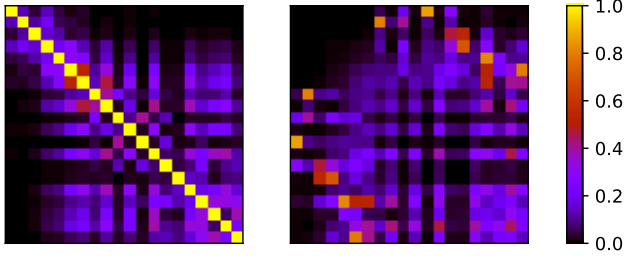


Fig. 5: Pairwise correlation (left) and pairwise pseudo-correlation (right) of the first twenty components of the SSA.

The off-diagonal pairwise correlations do not reach significant values, making difficult the pairing of LRR2 components. In contrast to that, the pseudo-correlation shows high pairwise values clearly allowing to group them and recover polarized LRR2 signals. This also illustrates that when the SSA singular vectors related to the original LRR2 signals are pseudo-correlated, then the SSA components in step 3 remain strongly pseudo-correlated.

5. EXPERIMENTAL RESULTS

An illustration of the ability of complex SSA with pseudo-correlation criterion to extract polarized components from a real signal is presented. The bivariate signal to be analyzed is given in Figure 1. It is a seismic recording from the 1991 Solomon Islands Earthquake, already studied in [17–19] and the data can be found at [13]. The original signal is trivariate, but most of the energy is contained in a 2D plane, i.e., the bivariate signal from Figure 1. The data was reduced to the tremor between samples 7000 and 11000, meaning that the length of the effectively processed signal is $N = 4000$. The window length of the SSA procedure is chosen as $L = \lfloor \frac{N}{4} \rfloor = 1000$. A rank of $r = 20$ was chosen for the SVD in step 1 (20 components kept), which corresponds to about 96% of the original signal energy.

Figure 5 presents the pairwise correlation and pseudo-correlation between the outputs of the third step of the SSA. The correlation map (left side of Figure 5) does not exhibit clear potential pairings. In contrast to that, strong pseudo-correlations (yellow dots on the right side map of Figure 5) indicate that several pairs of components can be grouped to form signals with polarization close to elliptical. This also means that they can be grouped into components with arguments rotating in opposite direction along time (known as rotary components [7, 12]).

Extraction of the two most pseudo-correlated components, the 1st and the 12th, leads to the bivariate signal presented in Figure 6 (as the other pairs of pseudo-correlated leading components have similar characteristics they are not shown for space reasons). It is the archetype of polarization component that can be obtained using complex SSA and the pseudo-correlation based grouping method. The elliptical polarization of this component can be seen on the left panel of Figure 6. It is a rank-2 polarized component, and provides an approximation of the original signal that only contains partial information on the polarization of the signal.

In order to estimate more accurately the polarized part of the signal, a rank-12 approximation was performed by summing the 6 most pseudo-correlated leading components (see Figure 5). The resulting bivariate signal is displayed in Figure 7. It represents 75% of the original signal RMS (Root Mean Square) and contains higher polarization diversity. The residual signal, obtained after subtraction

of the rank-12 approximation from the original signal is displayed in Figure 8. It consists in a combination of unpolarized signals that can potentially be referred as noise.

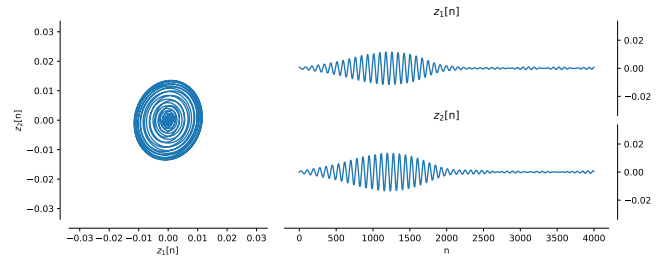


Fig. 6: 1st and 12th components of the complex SSA grouped using the pseudo-correlation criterion.

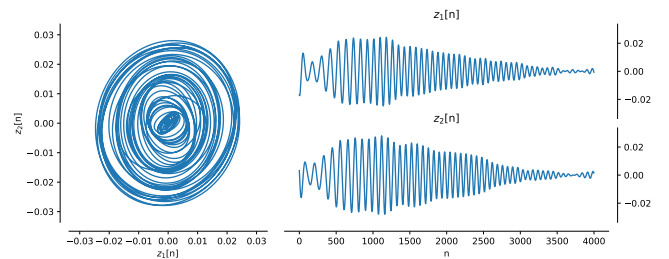


Fig. 7: Rank-12 approximation of the original signal using complex SSA and the pseudo-correlation criterion. Indexes of the grouped pairs are: (1, 12), (2, 8), (3, 14), (4, 15), (5, 17) and (6, 20). See pseudo-correlation map on the right-side of Figure 5.

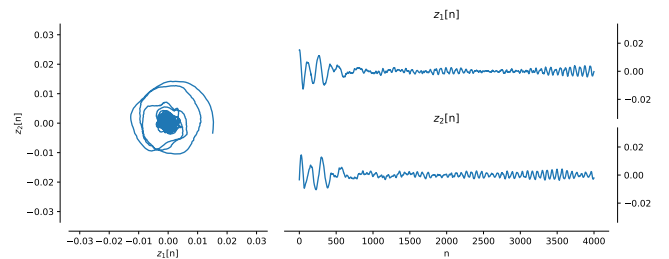


Fig. 8: Residual signal obtained from the subtraction of the rank-12 approximation (Figure 5) from the original signal (Figure 1).

6. CONCLUDING REMARKS

This paper demonstrates the advantages of using a pseudo-correlation criterion in the grouping step of the complex SSA pipeline. It allows to provide low-rank polarized approximations of bivariate signals and can perform polarized signal extraction and estimation in noisy scenarios, with applicability to real-world data. The constrained LRR2 are rank-2 bricks allowing to approximate polarized signals.

Future works will intend to generalize the proposed approach to analyze and process non-stationary polarized signals. This could be done either by considering constrained LRR2 with time varying coefficients, or by developing the notion of sliding polarized complex SSA, in the spirit of the methodology developed in [20] for non-stationary real-valued signals.

7. REFERENCES

- [1] C. Brosseau, “Fundamentals of polarized light : a statistical optics approach,” *Wiley-Interscience*, 1998.
- [2] W. Brown and R. Crane, “Conjugate linear filtering,” in *IEEE Transactions on Information Theory*, 1969, vol. 15, pp. 462 – 465.
- [3] J. Samson, “Pure states, polarized waves, and principal components in the spectra of multiple, geophysical time-series,” in *Geophysical Journal International*, 1983, vol. 72, pp. 647 – 664.
- [4] C. R. Pinnegar, “Polarization analysis and polarization filtering of three-component signals with the time-frequency,” in *Geophysical Journal International*, 2006, vol. 165, pp. 596 – 606.
- [5] B. P. Abbott et al., “Observation of gravitational waves from a binary black hole merger,” *Phys. Rev. Lett.*, vol. 116, 2016.
- [6] J. Flamant, P. Chainais, E. Chassande-Mottin, F. Feng, and N. Le Bihan, “Non-parametric characterization of gravitational-wave polarizations,” in *XXV European Signal Processing Conference. EUSIPCO*, 2018.
- [7] J. Gonella, “A rotary-component method for analyzing meteorological and oceanographic vector time series,” in *Deep Sea Research and Oceanographic Abstracts*, 1972, vol. 19, pp. 833 – 846.
- [8] R. E. Thomson and W. J. Emery, “Data analysis methods in physical oceanography, third edition,” *Elsevier Science*, 2014.
- [9] J. Flamant, N. Le Bihan, and P. Chainais, “Spectral analysis of stationary random bivariate signals,” *IEEE Transactions on Signal Processing*, vol. 65, no. 23, pp. 6135–6145, 2017.
- [10] J. Flamant, P. Chainais, and N. Le Bihan, “A complete framework for linear filtering of bivariate signals,” *IEEE Transactions on Signal Processing*, vol. 66, no. 17, pp. 4541–4552, Sept. 2018.
- [11] D. P. Mandic and V. S. L. Goh, “Complex valued nonlinear adaptive filters: Noncircularity, widely linear and neural models,” in *Wiley Series in Adaptive and Learning Systems for Signal Processing, Communications, and Control*, 2009, pp. 13–32.
- [12] P. J. Schreier and L. L. Scharf, “Statistical signal processing of complex-valued data: the theory of improper and noncircular signals,” *Cambridge University Press*, 2010.
- [13] J. M. Lilly, “Jlab: A data analysis package for matlab,” <http://www.jmlilly.net/jmlsoft.html>, 2016.
- [14] N. Golyandina, V. Nekrutkin, and A. Zhigljavsky, “Analysis of time series structure, SSA and related techniques,” *Chapman Hall/CRC*, 2001.
- [15] N. Golyandina, A. Korobeynikov, A. Shlemov, and K. Usevich, “Multivariate and 2d extensions of singular spectrum analysis with the RSSA package,” *arXiv preprint arXiv:1309.5050*, 2013.
- [16] N. Golyandina, A. Korobeynikov, and A. Zhigljavsky, “Singular spectrum analysis with R,” *Springer Berlin, Heidelberg*, 2018.
- [17] J. Flamant, N. Le Bihan, and P. Chainais, “Time-frequency analysis of bivariate signals,” *Applied and Computational Harmonic Analysis*, vol. 46, no. 2, pp. 351 – 383, 2019.
- [18] S. Olhede and A.T. Walden, “Polarization phase relationships via multiple Morse wavelets. I. Fundamentals,” in *Royal Society*, 2003, vol. 459, p. 413–444.
- [19] J. M. Lilly and J. Park, “Multiwavelet spectral and polarization analyses of seismic records,” *Geophysical Journal International*, vol. 122, pp. 1001–1021, 1995.
- [20] J. Harmouche, D. Fourer, F. Auger, P. Borgnat, and P. Flandrin, “The Sliding Singular Spectrum Analysis: A Data-Driven Nonstationary Signal Decomposition Tool,” *IEEE Transactions on Signal Processing*, vol. 66, no. 1, pp. 251–263, Jan. 2018.